Charge-ordering phase transition and order-disorder effects in the Raman spectra of NaV_2O_5

M.J.Konstantinović *
Simon Fraser University, Physics Department, 8888 University drive, Burnaby, B.C. V5A1S6 Canada
Max-Planck-Institut für Festkörperforschung, Heisenbergstr. 1, D-70569 Stuttgart, Germany

M.Isobe and Y.Ueda
Institute for Solid State Physics, The University of Tokio, 7-22-1 Roppongi, Minato-ku, Tokio 106, Japan

Abstract

In the ac polarized Raman spectra of NaV_2O_5 we have found anomalous phonon broadening, and an energy shift of the low-frequency mode as a function of the temperature. These effects are related to the breaking of translational symmetry, caused by electrical disorder that originates from the fluctuating nature of the $V^{4.5+}$ valence state of vanadium. The structural correlation length, obtained from comparisons between the measured and calculated Raman scattering spectra, diverges at $T < 5$ K, indicating the existence of the long-range charge order at very low temperatures, probably at $T = 0$ K.

PACS: 78.30.-j, 78.30.Ly, 64.60.Cn, 78.30.Hv

The investigation of the physical phenomena associated to the low-dimensional magnetic structures, like a spin-Peierls (SP) transition discovered in the inorganic compound $CuGeO_3$[1], are of great importance for better understanding of strong electron correlations. A very interesting interplay between spin and charge dynamics results in a phase transition discovered in NaV_2O_5[2,3]. At higher temperatures ($T > 34K$) the magnetic susceptibility of NaV_2O_5 is in excellent agreement with the Bonner-Fisher curve for the one-dimensional Heisenberg antiferromagnet. At low temperatures, however, the susceptibility decreases rapidly to zero[2] suggesting a SP transition at T=34 K. On the other hand, the temperature dependent nuclear magnetic resonance (NMR) spectra,[4] showed a change of the vanadium valence across the phase transition, from uniform $V^{4.5+}$ to two different V^{4+} and V^{5+} states. These measurements[2,4] gave direct evidence for the charge ordering (CO) phase-transition scenario in NaV_2O_5. A structural analysis,[5] and the polarized Raman and infrared (IR) spectra of NaV_2O_5[6], are also consistent with the existence of uniform vanadium valence in the high-temperature phase. However, despite extensive experimental and theoretical effort, no consistent picture has yet emerged for the low-temperature phase[7–20]. None of the models proposed to date, have explained fully the two intimately connected issues: the nature of the phase transition and the low-temperature ground state. Raman spectroscopy is a

powerful method for the study of dynamics of solids and it can be used to address these issues. Again, despite a considerable amount of data, the Raman spectra of NaV_2O_5 are still not completely understood[6,21]. This holds for the vibrational modes as well as for possible magnetic excitations.

In this report, we present the study of the vibrational modes in the Raman spectra of NaV_2O_5 and analysis of the effects associated with non conservation of the light-scattering wave vector selection rule $\mathbf{k}$=0. We argue that anomalous phonon broadening and frequency shifts, that are observed in the ac spectra as a function of the temperature, are caused by strong electrical disorder due to the fluctuating nature of the $V^{4.5+}$ valence state of vanadium. The temperature dependence of the structural correlation length is obtained from the comparison between measured and calculated Raman scattering spectra, and used to characterize the phase transition in NaV_2O_5. This analysis shows, that the phase transition at $T_c = 34K$ corresponds to the onset of the short-range electron correlations, with a true long-range order (CO) at $T \sim$0. Thus, the charge order is not static below Tc, in contrast to the conclusions of Lohmann et al[20].

Polarized Raman scattering experiments were performed on NaV_2O_5 single crystals (size $\sim 1 \times 3 \times 1$ mm^3 along **a**, **b**, and **c** respectively) prepared as described in Refs. 2 and 3. As an excitation source we used the 514.5 nm laser line from an Ar^+ ion laser. The beam, with an average power of 5 mW, was focused (spot diameter $\sim 80\mu$m) on the (001) and (101) surfaces of the crystals. The spectra were measured in a backscattering geometry using a DILOR triple monochromator equipped with a LN_2 cooled CCD camera. NaV_2O_5 crystallizes above T_c in the orthorombic centrosymmetric space group Pmmn (D_{2h}^{13}), with two molecules in the unit cell of a size: a=1.1318 nm, b=0.3611nm and c=0.4797 nm. Each vanadium atom, in the average valence state 4.5+, is surrounded by five oxygen atoms forming VO_5 pyramids. These pyramids are mutually connected via common edges and corners to form layers in the ab plane, see Fig. 1. The Na atoms are situated between these layers as intercalants. The structure of NaV_2O_5 can also be described as an array of parallel ladders (running along the **b** direction) coupled in a trellis lattice (each rung is made of a V-O-V bond).

The vibrational properties of NaV_2O_5 are studied in great details by measuring the Raman spectra only from (001) surface[6,21]. In our previous paper[10] we observed an interesting low-frequency structure in the ac scattering geometry which, as we will show below, exhibits an unusual temperature dependence. The polarized Raman scattering spectra from (001) and (101) planes, at temperatures above and below phase-transition temperature, are presented in Fig. 2. The **b** axis of the crystals is set to be parallel to the laboratory H horizontal) axis. Thus the VV (V equals vertical) polarized scattering geometry from the (101) plane gives the mixture of aa, cc, and ac contributions (upper spectra in Fig. 2). The VV polarized configuration from the (001) plane gives only aa contribution (lower spectra in Fig. 2). The corresponding HH spectra (gives the bb contribution for both planes) are found to be identical. In this way we were able to determine the ac contribution at very low frequencies, otherwise impossible to get. For example, the low quality of the (010) surface, prevent us from direct measurements of the low frequency scattering in the ac geometry.

In addition to the phonon modes, and a continuum centered at 650 cm^{-1} which belongs to the aa channel, we found three modes in the VV spectra obtained from the (101) planes (Fig. 2), that represent the ac contribution. Their detailed temperature dependencies are

shown in inset of Fig. 2. The lowest frequency ac mode is centered at about 107 cm^{-1}. The mode is asymmetric with a frequency cutoff around 120 cm^{-1} (Fig.2 and Fig.3b). As the temperature is decreased below T_c, the mode becomes more symmetric, and hardens by amount of 10 cm^{-1} [Fig. 2 and Fig. 3b]. The integrated intensity of this feature increases rapidly by the increasing temperature below T_c, and becomes constant for $T > T_c$ (Fig. 4). The temperature behavior of the frequency and the integrated intensity is similar to what is usually observed for a two-magnon mode[22]. However, the two-magnon origin of this mode can be ruled out since its energy (117 cm^{-1}) below the phase transition temperatures[13] is much smaller then $2\Delta_s \sim 160\ cm^{-1}$. The additional argument for excluding the two-magnon scattering process comes from observation of the mode at temperatures as high as $10 \times T_c$. At these temperatures the two-magnon mode should not be visible in the Raman spectra[22]. A one-magnon scattering process, and other magnetic-related scattering mechanisms, can be also eliminated since we did not find any change in the spectra in the magnetic fields up to 12 T.

Our analysis shows that this structure might be related to the low frequency phonon density of states, due to the breakdown of the $\mathbf{k}$=0 conservation rule in the light scattering process. In NaV_2O_5 the $V^{4.5+}$ valence state of vanadium causes the random nature of the coupling between the atomic displacements and the fluctuations of the dielectric susceptibility. Such randomness actually appears because of irregular atomic bonding. The visualization of randomness in NaV_2O_5 is schematically presented in Fig. 1 and it can be referred as an "electrical disorder",[23]. Imagine that we "freeze" the electrical configuration of the charges in the rungs of the ladders, at certain time in the high-temperature phase. We find random electron configurations among rungs, Fig.1b. The average value for all rung configurations gives the $V^{4.5+}$ in which the electron is shared by the V atom at the each end of a rung. Below the phase transition temperature the charges start to order, ($V^{4.5\pm\alpha}$, $\alpha \neq 0$) Fig. 1c, reaching complete "zig-zag"[24] order at T=0 ($\alpha = 0.5$), Fig. 1d. The "zig- zag" phase is presented as a real low-temperature geometry, even though there are some other proposed CO configurations[25,9]. It will be evident from our results that we were not able to discriminate among the various possible CO patterns, and Fig.1 must be regarded only as illustrative of the electrical disorder. However, the "zig-zag" charge order is consistent with observed phonons in the Raman and IR spectra of NaV_2O_5[10]. If so, even for the perfect plane-wave phonon, for example an acoustic or optical phonon with a finite wave vector $\mathbf{k}$, disorder of the atomic coupling allows inelastic scattering of light from this mode[26]. Then, the light scattering is expected to be proportional to the phonon density of states properly weighted by the coupling constant which is in fact a function of ω.

The light-scattering cross section is proportional to the Fourier transform of the correlation function of the polarizability fluctuations:

$$I_{i,j}(\omega) \sim \int\int dtd(\mathbf{r}_1 - \mathbf{r}_2) e^{i\omega t - i\mathbf{k}(\mathbf{r}_1 - \mathbf{r}_2)} < \delta\chi_i^*(\mathbf{r}_1, t)\delta\chi_j(\mathbf{r}_2, 0) >, \quad (1)$$

where $\mathbf{k} = \mathbf{k}_I - \mathbf{k}_S$ and $\omega = \omega_I - \omega_S$ are wavevector and frequency of phonon(s) that participate in the light scattering process. The $< ... >$ denotes the equilibrium expectation value.

For the ideal crystals, both energy and wavevector conservation rules are fulfilled, and the first-order Raman intensity of phonons is proportional to two delta functions, $\delta(\omega_I - \omega_S - \omega) \cdot \delta(\mathbf{k} - q)$.

In disordered crystals the **k**=0 selection rule is broken due to lack of the translational invariance, and the Stokes part of the Raman scattering intensity is $I(\omega)\omega/[1+n(\omega)] \sim \sum_j C_j(\omega)g_j(\omega)$. The $g_j(\omega)$ is a density of states for the band j, and the $n(\omega)$ is Bose distribution function[23]. $C_j(\omega)$ describes the coupling of the light and the vibrational mode ω. In a continuum description[23] the fluctuations of the susceptibility result from the elastic strain field $e_j(\omega, \mathbf{r}) = ke_j(\omega)exp(i\mathbf{kr})$ of the phonon (plane wave), which is modulated by static fluctuations $\delta p_{ik}(\mathbf{r})$ of the elasto-optical constants: $\delta\chi_i(\mathbf{r}) = -\epsilon^2/(4\pi)[p_{ij} + \delta p_{ij}(\mathbf{r})]e_j(\mathbf{r})$. In this way, the coupling constant $C(\omega) \sim k^2 \int drexp(i\mathbf{kr})F(\mathbf{r})$ is expressed as a correlation function $F(\mathbf{r})$ of the fluctuations δp of the elastoptical constants, which characterize the electrical disorder. The form of the correlations is usually postulated to be either exponential damping $exp(-r/l_c)$; or Gaussian damping $exp(-r^2/l_c^2)$, where l_c is correlation length. In the case of NaV_2O_5 we assume Gaussian damping to describe the electrical correlations. The correlation length may be defined as a length over which electrons in neighboring rungs "see" each other. In fact, this is just a positional (structural) correlation length. One simplified picture, where the intersite Coulomb interactions are "switched on" at T=34 K has been previously suggested[24].

Thus, the coupling constant is $C(\omega) \sim k^2 e^{-k^2 l_c^2/4}$. The ω dependence of $C(\omega)$ comes from the dispersion relation between the frequency and the wavevector [for example, if $\omega = ck$ then $C(\omega) = \omega/c)^2 exp[-(\omega/c)^2 l_c^2/4]$. The same type of the correlation function and the coupling constant have been obtained by Martin and Brenig[27] in their analysis of Brillouin scattering in the amorphous solids.

Finally, the normalized Raman intensity is:

$$I(\omega)\frac{\omega}{1+n(\omega)} \sim \sum_{\mathbf{k}} k^2 e^{-k^2 l_c^2/4}\delta[\omega - \omega(\mathbf{k})], \tag{2}$$

where $\omega(\mathbf{k})$ is a phonon dispersion. If we confine our analysis to the energy range of the acoustic or/and low frequency optical phonons ($\omega \leq 150$ cm^{-1}) the Raman spectrum in the high-T phase is influenced by two contributions: acoustic or optic phonon density of state contribution, $\sum_k \delta[\omega - \omega(\mathbf{k})]$ and the coupling function $C(k)$. Since dispersion curves of the phonons have not yet been measured, we are forced to make assumption about which phonons are involved in the light scattering process. There are two possibilities:

(a) Broad feature corresponds to the acoustic phonon with a zone-boundary energy of 117 cm^{-1}. Bellow T_c this mode is introduced to **k**=0 by zone folding effect. The x-ray diffraction experiments showed the existence of superlattice reflections below T_c with a lattice modulation vector **q**=(1/2, 1/2, 1/4)[13]. In this case the strong anomaly of the elastic constants is expected at T_c and indeed observed by Schwenk *et al.*[12].

(b) The mode corresponds to low-ω optical phonon, also allowed by the symmetry of the low-T phase, with energy that decreases as a function of the wavevector. According to the lattice dynamical calculations[28] a good candidate for that phonon could be the low-ω B_{2g} phonon (active in ac polarized geometry), with Na vibrations mainly along the **a** axis. By examining the Raman spectra it is difficult to conclude which one of these two assumptions is more appropriate, because of the strong quasi elastic background at low frequencies. However, this choice does not critically influence our conclusions, and for the sake of simplicity we assume the cos k form of the phonon dispersion, $\omega = \omega_0 cosk/2$, $\omega_0 = 117$ cm^{-1}, $k \in [0, \pi/a]$.

The calculated Raman spectra are presented in Fig. 3a and compared with measured ones, Fig 3b. Both the shift and the broadening of the mode are in good agreement with the experiment. The spectra are obtained by varying just one parameter l_c, evaluating equation 2 in one dimension, and by taking the values of k and l_c in appropriate units of a-lattice constant. By increasing temperature (from T=0), disorder is introduced and the contribution of the $C(k)$ in the spectra becomes important. The increase of the degree of disorder is produced by the increase of the $k \neq 0$ contributions, directed with $C(k)$. Therefore, the broadening of the mode and its energy shift towards lower energies are produced by decreasing l_c which is a measure of the degree of disorder; complete disorder is characterized with $l_c \sim$ a-interatomic distance and long range-order with $l_c = \infty$. The long-range order solution, $l_c = \infty$ and $C(k) = 0$ of equation 2, gives the vanishing of the Raman intensity. This is not unphysical. It is just telling us that one has to analyze the Raman spectra at T=0 using equation 1 instead of equation 2.

The peak position of the mode as a function of the temperature is shown in Fig. 4a. The circles (full lines) represent the experiment (theory). Since in our calculation of the Raman spectra the temperature does not enter as a parameter, the temperature dependence of the peak maximum is included only through the temperature dependence of the correlation length. It is generally expected that correlation length changes with temperature, and this dependence can be obtained by examining the phonon frequency change close to the phase transition-temperature. The best agreement between the measured and the calculated spectra is obtained by assuming a quadratic relation between the correlation length and the temperature, $1/l_c \sim T^2$. Therefore, the peak position can be used as a measure of disorder. Accordingly, a similar temperature dependence is expected for the order parameter α. Furthermore, we present the comparison between the temperature dependence of the measured and calculated integrated intensities, Fig. 4.b. Here, we also find very good agreement between theory and experiment using the same quadratic relation between $1/l_c$ and T, and by introducing a non zero intensity offset at T=0 K ($I(T = 0)/I(T = 100) = 0.3$).

The temperature dependence of the correlation length is presented in inset of Fig. 4. The particular value of lc that is used to calculate the Raman spectra, does not have deeper physical meaning because of an arbitrary factor in the exponent of equation 2. But its temperature dependence does. The correlation length has a approximately constant value above T_c and increases below T_c. This signals that the critical temperature $T_c = 34$ K represents the onset of short-range electron correlations. As the temperature is lowered below T_c, the correlation length rapidly increases indicating the existence of a possible singularity at temperatures below T=5 K. In this case the divergence of the correlation length corresponds to the appearance of the true long-range charge order at very low temperatures (probably at T=0). The short range electron correlations could correspond to intersite Coulomb interaction effects[24], which become important below 34 K, but the electron correlations should also persist in some form at temperatures above 34 K. Following the same arguments, the change of the spectral shape above 100 K (it is also found that some IR spectral changes occurs around 100 K,[7]) could be a consequence of an additional phase transition, magnetic in origin for example.

In conclusion, we have presented the evidence for the existence of translational symmetry breaking effects in the Raman spectra of NaV_2O_5. Non conservation of the light-scattering wave vector selection rule, $\mathbf{k} \approx 0$, is caused by strong electrical disorder due to the fluctuating

nature of the valence of vanadium. The temperature dependence of the structural correlation length has been obtained from the comparison between the measured and the calculated Raman scattering spectra. This suggests that the phase transition at $T_c = 34K$, represents the onset of the short range electron correlations, with true long-range order developing at $T \sim 0$.

Acknowledgments

MJK thanks to J.C.Irwin, I.Herbut and P.H.M. van Loosdrecht for helpful discussions and comments. This work is supported by Natural Sciences and Engineering Research Council of Canada. MJK also thanks to MPI-FKF Stuttgart, Germany for partial financial support.

*$mkonstan@sfu.ca$

REFERENCES

[1] M. Hase, I. Terasaki and K. Uchinokura, Phys. Rev. Lett. **70**, 3651 (1993).

[2] M. Isobe and Y. Ueda, J. Phys. Soc. Jpn. **65**, 1178 (1996); Y. Ueda and M. Isobe, J. Magn. Magn. Mat. **177**, 741 (1998).

[3] M. Isobe and Y. Ueda, J. of Alloys and Comp. **262**, 180 (1997).

[4] T. Ohama, H. Yasuoka, M. Isobe, and Y. Ueda, Phys. Rev B **59**, 3299 (1999).

[5] H. G. von Schnering Yu. Grin, M. Kaupp, M. Somer, R. K. Kremer, O. Jepsen, T. Chatterji, and M. Weiden, Zeit. Kristall. **213**, 246 (1998).

[6] M. Weiden, R. Hauptmann, C. Geibel, F. Steglich, M. Fischer, P. Lemmens, and G. Güntherodt, Z. Phys. B **103**, 1 (1997); Z. V. Popović, M. J. Konstantinović, R. Gajić, V. Popov, Y. S. Raptis, A. N. Vasil'ev, M. Isobe, and Y. Ueda, J. Phys. Cond. Matter **10**, L513 (1998); H. Kuroe, H. Seto, J. Sasaki, T. Sekine, M. Isobe, and Y. Ueda, J. Phys. Soc. Jpn. **67**, 2881 (1998).

[7] A. Damascelli, D. van der Marel, M. Grüninger C. Presura, T. T. M. Palstra, J. Jegoudez, and A. Revcolevschi, Phys Rev Lett. **81**, 918 (1998).

[8] A. N. Vasil'ev, V. V. Pryadun, D. I. Khomskii, G. Dhalenne, A. Revcolevschi, M. Isobe , and Y. Ueda, Phys. Rev. Lett. **81**, 1949 (1998).

[9] J. Lüdecke, A. Jobst, S. van Smaalen, E. Morré, C. Geibel, and H. G. Krane, Phys. Rev. Lett. **82**, 3633 (1999).

[10] M. J. Konstantinović, Z. V. Popović, M. Isobe, and Y. Ueda, Solid State Comm. **112**, 397 (1999).

[11] A. I. Smirnov, M. N. Popova, A. B. Sushkov, S. A. Golubchik, D. I. Khomskii, M. V. Mostovoy, A. N. Vasil'ev, M. Isobe, and Y. Ueda, Phys. Rev. B **59**, 14546 (1999).

[12] H. Schwenk, S. Zherlitsyin, B. Lüthi, E. Morré, and C. Geibel, Phys. Rev. B **60**, 9194 (1999).

[13] T. Yosihama, M. Nishi, K. Nakajama, K. Kakurai, Y. Fujii, M. Isobe, C. Kagami, and Y. Ueda, J. Phys. Soc. Jpn. **67**, 744 (1998).

[14] V. N. Vasil'ev, A. I. Smirnov, M. Isobe, and Y. Ueda, Phys. Rev. B **56**, 5065 (1997).

[15] S. G. Bompadre, A. F. Hebard, V. N. Kotov, D. Hall, G. Maris, J. Baas, and T. T. M. Palstra, Phys. Rev. B **61**, R13321 (2000).

[16] H. Smolinski, C. Gros, W. Weber, U. Peuchert, G. Roth, M. Weiden, and C. Geibel, Phys. Rev. Lett. **80**, 5164 (1998).

[17] C. Gros and R. Valentí, Phys. Rev. Lett. **82**, 976 (1999).

[18] B. D. Gaulin, M. D. Lumsden, R. K. Kremer, M. A. Lumsden, and H. Dabkowska, Phys. Rev. Lett. **84**, 3446 (2000).

[19] Y. Fagot-Rauvrat, M. Mehring, and R. K. Kremer, Phys. Rev. Lett. **84**, 4176 (2000).

[20] M. Lohmann, H. A. K. von Nidda, M. V. Eremin, A. Loidl, G. Obermeier, and S. Horn, Phys. Rev. Lett. **85**, 1742 (2000).

[21] M. Fischer, P. Lemmens, G. Els, G. Güntherodt, E. Ya. Sherman, E. Morré, C. Geibel, and F. Steglich, Phys. Rev. B **60**, 7284 (1999).

[22] see for example, M. G. Cottam and D. J. Lockwood in "Light scattering in Magnetic Solids", (John Wiley and Sons, New York 1986).

[23] J. Jäckle, in Amorphous Solids, edited by W. A. Phillips (Springer-Verlag, Berlin 1981).

[24] H. Seo and H. Fukujama, J. Phys. Soc. Jpn. **67**, 2602 (1998).

[25] P. Thalmeier and P. Fulde, Europhys. Lett. **44**, 242 (1998).

[26] R. Shuker and R. W. Gammon, Phys. Rev. Lett. **25**, 222 (1970).
[27] A. J. Martin and W. Brenig, Phys. Stat. Sol. B **64**, 163 (1974).
[28] Z. V. Popović, M. J. Konstantinović, R. Gajić, V. Popov, Y. S. Raptis, A. N. Vasil'ev, M. Isobe, and Y. Ueda, Solid State Comm. **110**, 381 (1999).

FIGURES

FIG. 1. a) Schematic representation of the NaV_2O_5 crystal structure in the (001) plane. The full circles represent oxigens, the small (large) circles represent vanadium (sodium) atoms. Schematic representation of the electrical disorder (order) at b) $T > T_c$, c) $T < T_c$, d) T=0 in the vanadium-oxygen ladders of NaV_2O_5. Each rung in the ladders represents the V-O-V bond with one electron (black dot).

FIG. 2. The polarized Raman scattering spectra of NaV_2O_5 at 300 K (thin line) and at 10 K (thick line), measured from (001) surface (lower spectra) and (101) surface (upper spectra). Arrows represent modes associated with the ac polarized contribution, see text. Inset: The temperature dependent (aa+cc+ac) Raman scattering spectra.

FIG. 3. The a) calculated and b) measured Raman scattering spectra in 50 to 130 cm^{-1} frequency range at various temperatures.

FIG. 4. The a) frequency and b) normalized integrated intensity of the 117 cm^{-1} mode as a function of the temperature. The circles (full lines) represent the measurements (theory). The dashed line is guide to an eye. Inset: The temperature dependence of the correlation length.

M.J.Konstantinovic et al. Fig. 1

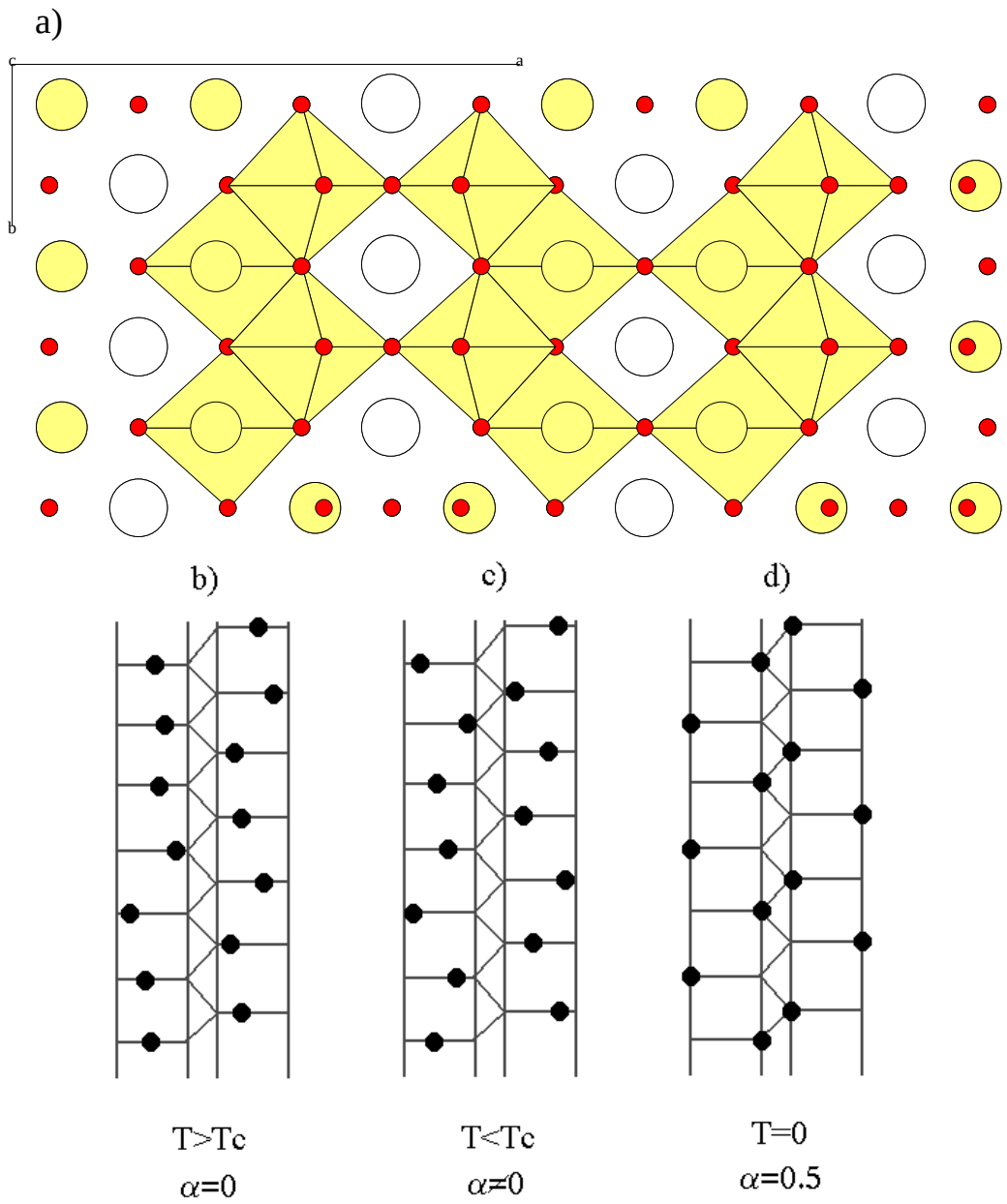

Konstantinovic et al. Fig. 2

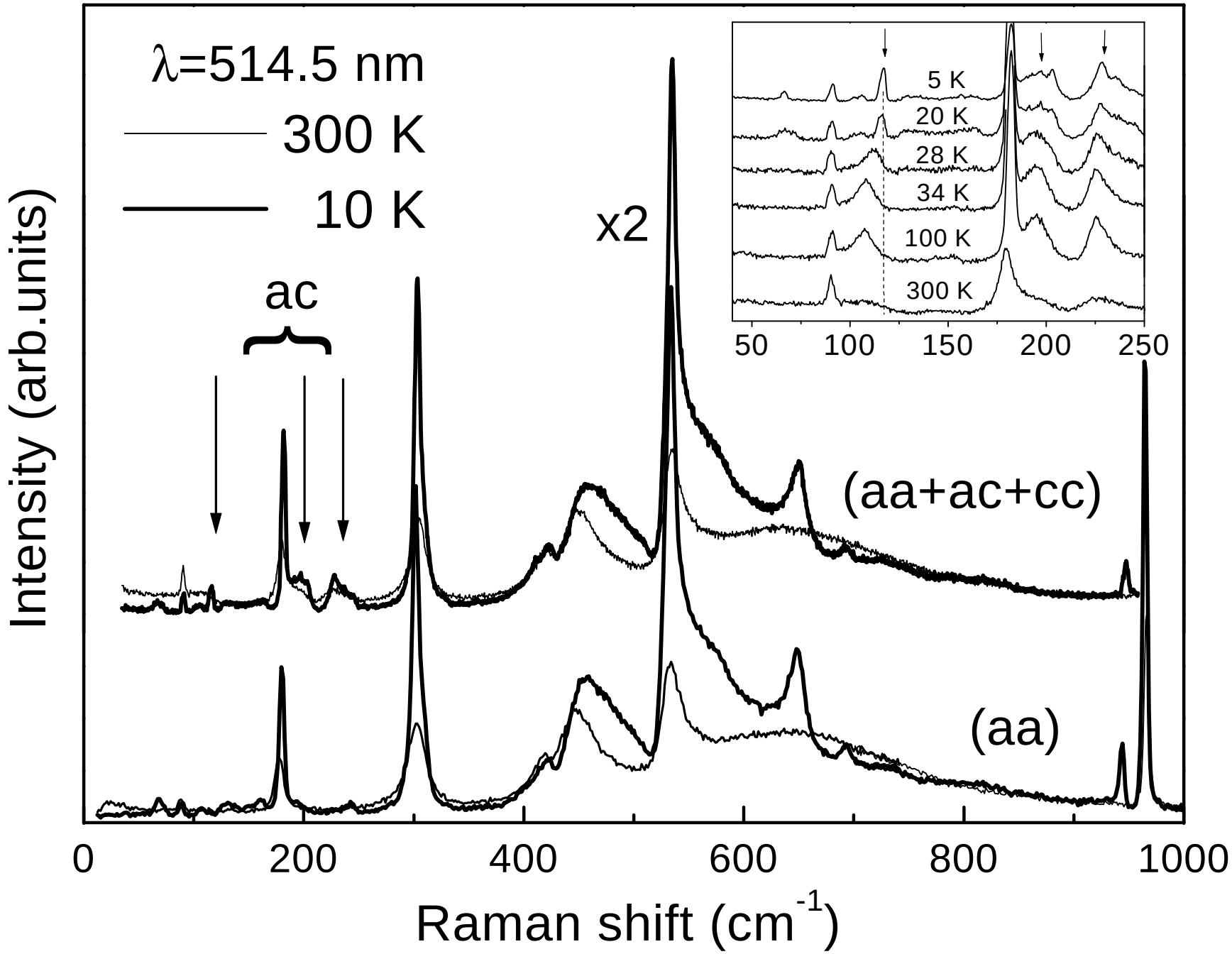

M.J.Konstantinovic et al. Fig. 3

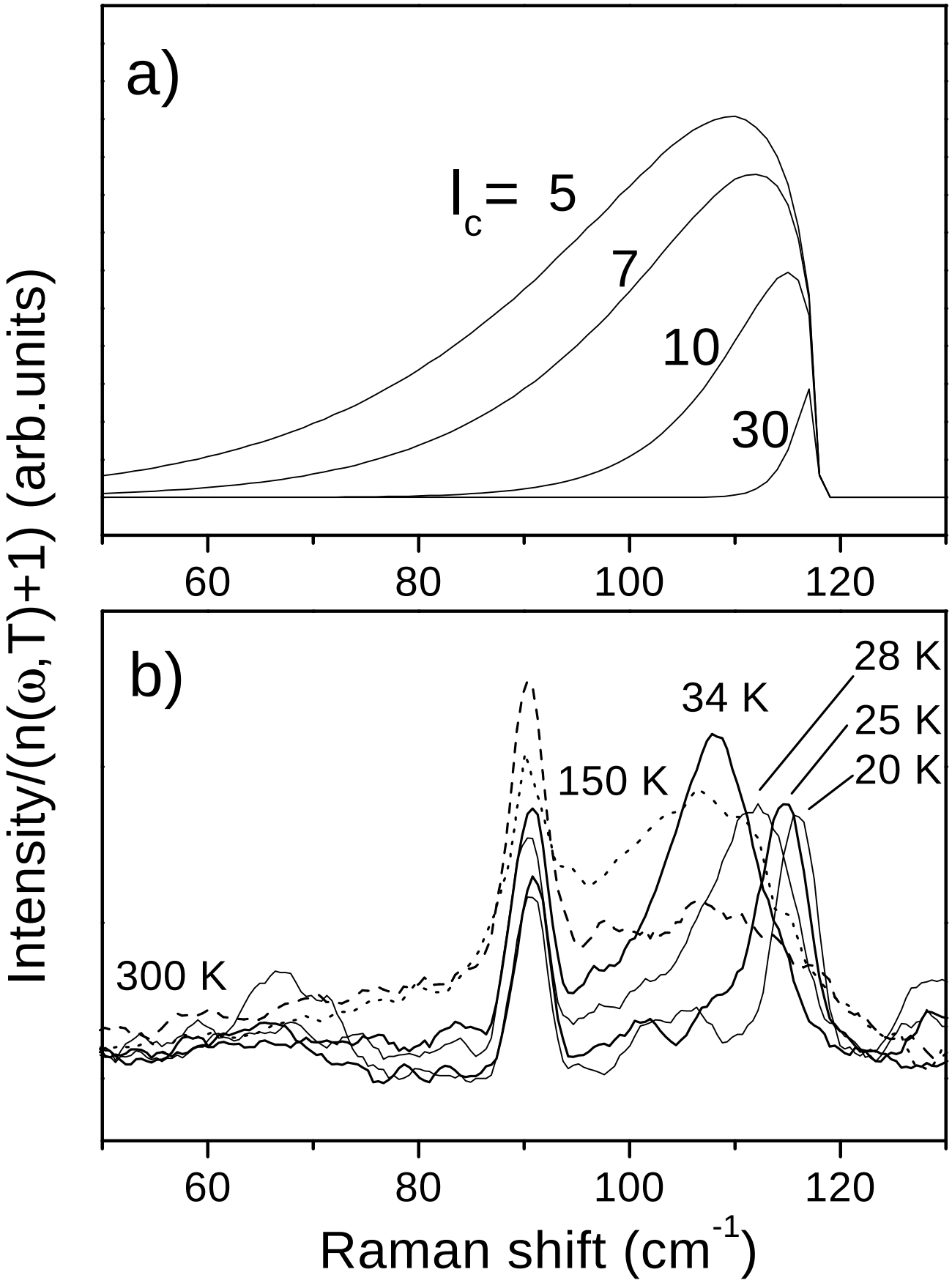

Konstantinovic et al. Fig.4